
WrapNet: Neural Net Inference with Ultra-Low-Resolution Arithmetic

Renkun Ni
University of Maryland
rn9zm@cs.umd.edu

Hong-min Chu
University of Maryland
hmchu@cs.umd.edu

Oscar Castañeda
Cornell University
oc66@cornell.edu

Ping-yeh Chiang
University of Maryland
pchiang@cs.umd.edu

Christoph Studer
Cornell University
studer@cornell.edu

Tom Goldstein
University of Maryland
tomg@cs.umd.edu

Abstract

Low-resolution neural networks represent both weights and activations with few bits, drastically reducing the multiplication complexity. Nonetheless, these products are accumulated using high-resolution (typically 32-bit) additions, an operation that dominates the arithmetic complexity of inference when using extreme quantization (e.g., binary weights). To further optimize inference, we propose a method that adapts neural networks to use low-resolution (8-bit) additions in the accumulators, achieving classification accuracy comparable to their 32-bit counterparts. We achieve resilience to low-resolution accumulation by inserting a cyclic activation layer, as well as an overflow penalty regularizer. We demonstrate the efficacy of our approach on both software and hardware platforms.

1 Introduction

Significant progress has been made in quantizing (or even binarizing) neural networks, and numerous methods have been proposed that reduce the precision of weights, activations, and even gradients while retaining high accuracy [3, 4, 6, 8, 10, 12, 14, 16–18, 23, 26, 28–30]. Such quantization strategies make neural networks more hardware-friendly by leveraging fast, integer-only arithmetic, replacing multiplications with simple bit-wise operations, and reducing memory requirements and bandwidth.

Unfortunately, the gains from quantization are limited as much of the computation in quantized networks still requires high-resolution arithmetic. Even if weights and activations are represented with just one bit, deep feature computation requires the summation of hundreds or even thousands of products. Performing these summations with low-resolution registers results in integer overflow, contaminating downstream computations and destroying accuracy. Moreover, as multiplication costs are slashed by quantization, high-resolution accumulation starts to dominate the arithmetic cost. Indeed, our own hardware implementations show that an $8\text{-bit} \times 8\text{-bit}$ multiplier consumes comparable power and silicon area to a 32-bit accumulator. When reducing the resolution to a $3\text{-bit} \times 1\text{-bit}$ multiplier, a 32-bit accumulator consumes more than $10\times$ higher power and area; see Section 4.5. Evidently, low-resolution accumulators are the key to further accelerating quantized nets.

In custom hardware, low-resolution accumulators reduce area and power requirements while boosting throughput. On general-purpose processors, where registers have fixed size, low-resolution accumulators are exploited through *bit-packing*, i.e., by representing multiple low-resolution integers side-by-side within a single high-resolution register [2, 22, 23]. Then, a single vector instruction is used to perform the same operation across all of the packed numbers. For example, a 64-bit register can be used to execute eight parallel 8-bit additions, thus increasing the throughput of software

implementations. Hence, the use of low-resolution accumulators is advantageous for both hardware and software implementations, provided that integer overflow does not contaminate results.

We propose WrapNet, a network architecture with extremely low-resolution accumulators. WrapNet exploits the fact that integer computer arithmetic is cyclic, i.e, numbers are accumulated until they reach the maximum representable integer and then “wrap around” to the smallest representable integer. To deal with such integer overflows, we place a differentiable cyclic (periodic) activation function immediately after the convolution (or linear) operation, with period equal to the difference between the maximum and minimum representable integer. This strategy makes neural networks resilient to overflow as the activations of neurons are unaffected by overflows during convolution.

We explore several directions with WrapNet. On the software side, we consider the use of bit-packing for processors with or without dedicated vector instructions. In the absence of vector instructions, overflows in one packed integer may produce a carry bit that contaminates its neighboring value. We propose training regularizers that minimize the effects of such contamination artifacts, resulting in networks that leverage bit-packed computation with very little impact on final accuracy. For processors with vector instructions, we modify the bit-packed Gemmlowp library [1] to operate with 8-bit accumulators. Our implementation achieves up to $2.4\times$ speed-up compared to a 32-bit accumulator implementation, even when lacking specialized instructions for 8-bit multiply-accumulate. We also demonstrate the efficacy of WrapNet in terms of cycle time, area, and energy efficiency when considering custom hardware designs in a commercial 28 nm CMOS technology.

2 Related Work and Background

2.1 Network Quantization

Network quantization aims at accelerating inference by using low-resolution arithmetic. In its most extreme form, weights and activations are both quantized using binary or ternary quantizers. The binary quantizer Q_b corresponds to the sign function, whereas the ternary quantizer Q_t maps some values to zero. Multiplications in binarized or ternarized networks [5, 12, 18, 23, 29] can be implemented using bit-wise logic, leading to impressive acceleration. However, training such networks is challenging since fewer than 2 bits are used to represent activations and weights, resulting in a dramatic impact on accuracy compared to full-precision models.

Binary and ternary networks are generalized to higher resolution via uniform quantization, which has been shown to result in efficient hardware [13]. The multi-bit uniform quantizer Q_u is given by:

$$Q_u(x) = \text{round}(x/\Delta_x)\Delta_x, \tag{1}$$

where Δ_x denotes the quantization step-size. The output of the quantizer is a floating-point number x that can be expressed as $x = \Delta_x x_q$, where x_q is the fixed-point representation of x . The fixed-point number x_q has a “resolution” or “bitwidth,” which is the number of bits used to represent it. Note that the range of floating-point numbers representable by the uniform quantizer Q_u depends on both the quantization step-size Δ_x and the quantization resolution. Nonetheless, the number of different values that can be represented by the same quantizer depends only on the resolution.

Applying uniform quantization to both weights $w = \Delta_w w_q$ and activations $x = \Delta_x x_q$ simplifies computations, as an inner-product simply becomes

$$z = \sum_i w_i x_i = \sum_i (\Delta_w (w_q)_i) (\Delta_x (x_q)_i) = (\Delta_w \Delta_x) \sum_i (w_q)_i (x_q)_i = \Delta_z z_q. \tag{2}$$

The key advantage of uniform quantization is that the core computation $\sum_i (w_q)_i (x_q)_i$ can be carried out using fixed-point (i.e., integer) arithmetic only. Results in [4, 10, 14, 20, 21, 26, 30] have shown that high classification accuracy is attainable with low-bitwidth uniform quantization, such as 2 or 3 bits. Although $(w_q)_i$, $(x_q)_i$, and their product may have extremely low-resolution, the accumulated result z_q of many of these products has very high dynamic range. As a result, high-resolution accumulators are typically required to avoid overflows, which is the bottleneck for further arithmetic speedups.

2.2 Low-Resolution Accumulation

Several approaches have been proposed that use accumulators with fewer bits to obtain speedups. For example, reference [9] splits the weights into two separate matrices, one with small-

Table 1: Average overflow rate (in 8 bits) of each layer for a low-resolution network and corresponding test accuracy using either 32-bit or 8-bit accumulators during inference.

Bit (A/W)	Overflow rate (8-bit)	Accuracy (32-bit)	Accuracy (8-bit)
full precision	–	92.45%	–
3/1	10.84%	91.08%	10.06%
2/1	1.72%	88.46%	44.04%

and another with large-magnitude entries. If the latter matrix is sparse, acceleration is attained as most computations rely on fast, low-resolution operations. However, to significantly reduce the accumulator’s resolution, one would need to severely decrease the magnitude of the entries of the first matrix, which would, in turn, prevent the second matrix from being sufficiently sparse to achieve acceleration. Recently, reference [7] proposed using layer-dependent quantization parameters to avoid overflowing accumulators with fixed resolution. Fine-tuning is then used to improve performance. However, if the accumulator resolution is too low (e.g., 8 bits or less), the optimized resolution of activations and weights is too coarse to attain satisfactory performance. Another line of work [19, 24, 27] uses 16-bit floating-point accumulators for training and inference—such approaches typically require higher complexity than methods based on fixed-point arithmetic.

2.3 The Impact of Integer Overflow

Overflow is a major problem, especially in highly quantized networks. Table 1 demonstrates that overflows occur in around 11% of the neurons in a network with binary weights (W) and 3-bit quantized activations (A) that is using 8-bit accumulators for inference after being trained on CIFAR-10 with standard precision. Clearly, overflow has a significant negative impact on accuracy. Table 1 shows that if we use an 8-bit (instead of a 32-bit) accumulator, then the accuracy of a binary-weight network with 2-bit activations drops by more than 40%, even when only 1.72% neurons overflow. If we repeat the experiment with 3-bit activations and binary weights, the final accuracy is only marginally better than a random guess. As a result, existing methods try to *avoid* integer overflow by using accumulators with relatively high resolution, and pay a correspondingly high price when doing arithmetic.

3 WrapNet: Dealing with Integer Overflows

We now introduce WrapNet, which includes a cyclic activation function and an overflow penalty, enabling neural networks to use low-resolution accumulators. We also present a modified quantization step-size selection strategy for activations, which retains high classification accuracy. Finally, we show how further speed-ups can be achieved on processors with or without specialized vector instructions.

We propose training a network with layers that emulate integer overflows on the fixed-point pre-activations z_q to maintain high accuracy. However, directly training a quantized network with an overflowing accumulator diverges (see Table 2) due to the discontinuity of the modulo operation. To facilitate training, we insert a cyclic “smooth modulo” activation immediately after every linear/convolutional layer, which not only captures the wrap-around behavior of overflows, but also ensures that the activation is continuous everywhere. The proposed smooth modulo activation c is a composite function of a modulo function m and a basis function f that ensures continuity. Specifically, given a b -bit accumulator, our smooth-modulo c for fixed-point inputs is as follows:

$$f(m) = \begin{cases} m, & \text{for } -\frac{k}{k+1}2^{b-1} \leq m \leq \frac{k}{k+1}2^{b-1} \\ -k2^{b-1} - km, & \text{for } m < -\frac{k}{k+1}2^{b-1} \\ k2^{b-1} - km, & \text{for } m > \frac{k}{k+1}2^{b-1} \end{cases}$$

$$c(z_q) = f(\text{mod}(z_q + 2^{b-1}, 2^b) - 2^{b-1}),$$

where k is a hyper-parameter that controls the slope of the transition. Note that we apply constant shifts to keep the input of f in $[-2^{b-1}, 2^{b-1})$. Figure 1a illustrates the smooth modulo function with two different transition slopes $k = 1, 4$. As k increases, the cyclic activation becomes more similar to the modulo operator and has a greater range, but the transition becomes more abrupt.

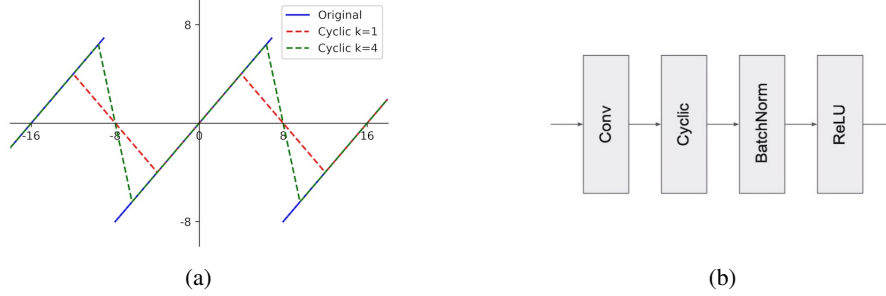


Figure 1: (a) Example of the proposed cyclic activation with different slopes k and the original modulo operator for a 4-bit accumulator. (b) Convolutional block with proposed cyclic activation.

Note that, since our cyclic activation is continuous and differentiable almost everywhere, standard gradient-based learning can be applied easily. A convolutional block with cyclic activation layer is shown in Figure 1b. After the convolution result goes into the cyclic activation, the result is multiplied by Δ_z to compute a floating-point number, which is then processed through BatchNorm and ReLU. A fixed per-layer quantization step-size is then used to convert the floating-point output of the ReLU into a fixed-point input for the next layer. We detail the procedure to find this step-size in Section 3.2.

3.1 Overflow Penalty

An alternative way to adapt quantized networks to low-resolution accumulators is to directly reduce the amount of overflows. To achieve this, we propose a regularizer which penalizes outputs that exceed the bitwidth of the accumulation register. Concretely, for a b -bit accumulator, we define an overflow penalty for the l -th layer of the network as follows:

$$R_l^o = \frac{1}{N} \sum_i \max\{|z_q^i| - 2^{b-1}, 0\}.$$

Here, z_q^i is the fixed-point result in (2) for the i -th neuron of the l -th layer, and N is the total number of neurons in the l -th layer. The overflow penalty is imposed after every quantized linear layer and before the cyclic activation. All these penalties are combined into one regularizer $R^o = \sum_l R_l^o$.

3.2 Selection of Activation Quantization Step-Size

To keep multiplication simple, the floating-point output of ReLU must be quantized before it is fed into the following layer. However, as shown in Table 1, a significant number of overflow occurs even with 3-bit activations. From our experiments (see Table 3), we have observed that if overflow occurs too frequently (i.e., on more than 10% of the neurons), then WrapNet starts to suffer significant accuracy degradation. However, if we reduce the activation resolution so that no overflows happen at all, several layers will have 1-bit activations (see Table 3), thereby increasing quantization errors and degrading accuracy. To balance accumulation and quantization errors, we adjust the quantization step-size Δ_x of each layer based on the overflow rate, i.e., the percentage $p\%$ of neurons that overflow in the network. If the overflow rate $p\%$ is too large, then we increase the quantization step-size Δ_x to reduce the overflow rate $p\%$. The selected quantization step-size is then fixed for further fine-tuning.

3.3 Adapting to Bit-Packing

Most modern processors provide vector instructions that enable parallel operation on multiple 8-bit numbers. For instance, the AVX2 (NEON) instruction set on x86 (ARM) processors provides parallel processing with 32 (16) 8-bit numbers. Vector instructions provide a clean implementation of bit-packing, which WrapNet can leverage to attain significant speed-ups.

While some embedded processors and legacy chips do not provide vector instructions, bit-packing can still be applied. Without vector instructions for multiplication, binary/ternary weights must be used to replace multiplication with bit-wise logic [2, 22]. Furthermore, bit-packing of additions is more delicate: Each integer overflow not only results in wrap-around behavior, but also generates a carry

bit that contaminates the adjacent number—specialized vector instructions avoid such contamination. We propose the following strategies to minimize the impact of carry propagation.

Reducing variance in the number of carries. The number of carries generated during a convolution operation can be large. Nevertheless, if we can keep the number of carries approximately the same for all the neurons among a batch of images, the estimated number of carries can be subtracted from the result to correct the outputs of a bit-packed convolution operation. To achieve this, during training, we calculate the number of carries for each neuron and impose a regularizer, R^c , to keep the variance of the number of carries small. The detailed formulation of R^c can be found in Appendix A.1.

Using a buffer bit. Alternatively, since each addition can generate at most one carry bit, we can place a buffer bit between every low-bit number in the bit-packing. For example, instead of packing eight 8-bit representations into a 64-bit number, we pack eight 7-bit numbers with one buffer bit between each of them. These buffer bits absorb the carry bits, and are cleared using bit-wise logic after each addition. Buffering makes representations 1-bit smaller, which potentially degrades accuracy.

A hybrid approach. To get the benefits from both strategies, we use a variance penalty on layers that have small standard deviation to begin with, and equip the remaining layers with a buffer bit.

4 Experiments

We compare the accuracy and efficiency of WrapNet to networks with full-precision accumulators using the CIFAR-10 and ImageNet benchmark datasets. Most experiments use binary or ternary weights for WrapNet as AVX2 lacks 8-bit multiplication instructions, but supports 8-bit additions and logic operations needed for binary/ternary convolutions.

4.1 Training Pipeline

We first pre-train a network with quantized weights and no cyclic layers, while keeping full-precision activations. Then, we select the quantization step-sizes of the activations (see Section 3.2) such that each layer has an overflow rate of around $p\%$ (a hyper-parameter) with respect to the desired accumulator bitwidth. Given the selected quantization step-size for each layer and the pre-trained network, we insert our proposed cyclic activation layer. We then warm-up our WrapNet by fine-tuning with full-precision activation for several epochs. Finally we further fine-tune the network with both activations and weights quantized. Both overflow and carry variance regularizers are only applied in the final fine-tuning step, except when training ResNet for ImageNet, where the regularizers are also included during warm-up. We leave the first and last layer at full-precision as in [23, 28].

4.2 Adapting to Low-Resolution Accumulators

We conduct ablation studies on the following factors: the type of cyclic function, the initial overflow rate for quantization step-size and resolution selection, and the coefficient of the overflow penalty regularizer. These experiments are conducted on a small VGG-7 [16] network, which is commonly used in the quantization literature for CIFAR-10. We binarize the weights as in [23], and we train WrapNet to adapt to an 8-bit accumulator. Our ablations change only one factor at a time while keeping the other factors fixed. As our default hyper-parameter setting, we use $k = 2$ as the transition slope, $p = 5\%$ as the initial overflow rate, and 0 as the coefficient for the regularizer.

Cyclic activation function. We compare the performance of various transition slopes k of our cyclic function c in Table 2, and we achieve the best performance when $k = 2$. If k is too small, then the accuracy decreases due to a narrower effective bitwidth (only half of the bitwidth is used when $k = 1$). Meanwhile, the abrupt transition for large k hurts the performance as well. In the extreme case where the cyclic function degenerates to modulo ($k \rightarrow \infty$), WrapNet diverges to random guessing, which highlights the importance of training with a “smooth” cyclic non-linearity to assimilate integer overflow. We also experimented with other choices of the cyclic function, such as a “V”-shaped cyclic absolute value function. However, they performed worse than the proposed cyclic function. We also find that placing a ReLU after batch norm yields the best performance, even though the cyclic function is already non linear. More experimental results can be found in Appendix B.1.

Quantization step-size. As described in Section 3.2, the quantization step-sizes are selected to balance the rounding error of the activations and accumulation errors due to overflow. We compare

Table 2: Results for different transition slopes for cyclic function; * denotes divergence.

k	1	2	4	10	∞
Accuracy	90.24%	90.52%	90.25%	89.16%	*

Table 3: Results for different quantization step-sizes based on overflow rate $p(\%)$. * denotes divergence.

p	Bits	Accuracy	p	Bits	Accuracy
0	1	90.07%	20	4	88.25%
2	3	90.51%	30	5	85.30%
5	3	90.52%	40	5	36.11%
10	4	89.92%	50	5	*

Table 4: Results for fine-tuning with the overflow penalty (R^o).

R^o	$p\%$	Accuracy	Difference
0	20	88.25%	–
0	5	90.52%	2.27%
0.01	20	90.05%	–
0.01	5	90.81%	0.76%

the classification performance when we choose different step-sizes to control the overflow rate as in Table 3. If the initial overflow rate is large, then the quantization step-size will be finer, but training is less stable. We obtain the best performance when the initial overflow rate is around 5%. The median bitwidths of the activations across layers are also reported in Table 3. Note that if we want to suppress all overflows, we can only use 1-bit activations. We also observe that WrapNet can attain reasonable accuracy (85%) even with a large overflow rate (around 30%), which demonstrates that our proposed cyclic activations provides resilience against integer overflows.

Overflow penalty. The overflow penalty regularizer improves stability to step-size selection. More specifically, in Table 4, the difference in accuracy between two step-size selections decreases from 2.27% to 0.76% after adding the regularizer. The overflow penalty also complements our cyclic activation, as we achieve the best performance when using both of them together during the fine-tuning stage. Moreover, in Appendix B.2, we compare our results to fine-tuning the pre-trained network using the overflow regularizer only. In the absence of a cyclic layer, neural networks still suffer from low accuracy (as in Section 2.3) unless a very strong penalty is imposed.

4.3 Adapting to Bit-Packing

We now show the efficacy of WrapNet for bit-packing without vector operations. We use the same architecture, binary weights, 8-bit accumulators, and hyper-parameters as in Section 4.2. The training details can be found in Appendix A.2. We consider CIFAR-10, and we compare with the best result of WrapNet from the previous section as a baseline. Without specific vector instructions, accuracy degenerates to a random guess because of undesired carry contamination during inference.

Surprisingly, with the carry variance regularizer, WrapNet works well even with abundant carry contamination during inference (for each neuron, 384 on average over all the dataset). The regularizer drops the standard deviation of the per-neuron carry contamination by 90%. When we use the hybrid approach, the accuracy is further improved (89.43%) and close to the best result (90.81%) we can achieve with vector instructions that do not propagate carries across different numbers (see Table 5).

Table 5: Results for adaptation to bit-packing with 8-bit accumulator. (v) denotes no carry contamination as in a vector instruction; (c) denotes carry propagation between different numbers.

Method	Accuracy (v)	Accuracy (c)	Carry	Carry Std
Baseline	90.81%	10.03%	254.91	159.55
Buffer Bit	–	88.22%	–	–
R^c	–	87.86%	384.42	17.91
Hybrid	–	89.43%	482.4	16.18

4.4 Benchmark Results

In this section, we compare our WrapNet when there is no carry contamination, with the following 32-bit accumulator baselines: a full-precision network (FP), a network trained with binary/ternary weights but with full-precision activations (BWN/TWN), and a network where both weights and activations are quantized to the same resolution as our WrapNet (BWN/TWN-QA). We benchmark our results on both CIFAR-10 and ImageNet. We use VGG7 and ResNet-20 for our CIFAR-10 experiments, and we use AlexNet [15, 25] and ResNet-18 [11] for our ImageNet experiments. Details of training can be found in Appendix B.3.

For CIFAR-10, even with an 8-bit accumulator, our results are comparable (less than 1% difference) to both BWN and TWN. When adapting to a 12-bit accumulator, we further achieve performance on-par with TWN and better than BWN (see Table 6).

For ImageNet, our WrapNet can achieve accuracy as good as BWN and TWN when adapting to a 12-bit accumulator where we can use roughly 7-bit quantized activations. However, in the extreme low-resolution case (8-bit accumulator), the accuracy of our binary WrapNet drops around 8% due to the limited bitwidth we can use for activations. As reported in Table 6, the median activation bitwidth is roughly 3-bit, and for some layers in AlexNet, we can only use 1-bit activations. Despite the gap from BWN, we observe that our model can achieve almost the same as performance as BWN-QA where the same resolution is used for activations. When using ternary weights, our WrapNet only drops by 2% from TWN for ResNet18, even when using an 8-bit accumulator.

Table 6: Top-1 test accuracy for both CIFAR-10 and ImageNet with different architectures. Here, “Acc” represents accumulator, and “QA” represents quantized activation.

	Bits			CIFAR-10		ImageNet	
	Activation	Weight	Acc	VGG7	ResNet20	AlexNet	ResNet18
FP	32	32	32	92.45%	91.78%	60.61%	69.59%
BWN	32	1	32	91.55%	90.03%	56.56%	63.55%
BWN-QA	~ 3	1	32	91.30%	89.86%	46.30%	57.54%
WrapNet	~ 3	1	8	90.81%	89.78%	44.88%	55.60%
WrapNet	~ 7	1	12	91.59%	90.17%	56.62%	63.11%
TWN	32	2	32	91.56%	90.36%	57.57%	65.70%
TWN-QA	~ 4	2	32	91.49%	90.12%	55.84%	63.67%
WrapNet	~ 4	2	8	91.14%	89.56%	52.24%	62.13%
WrapNet	~ 7	2	12	91.53%	90.88%	57.60%	63.84%

4.5 Efficiency Analysis

We conduct an efficiency analysis of parallelization by bit-packing, both with and without vector operations, on an Intel i7-7700HQ CPU operating at 2.80 GHz. We also conduct a detailed study of improvements that can be obtained using custom hardware.

AVX2 instruction efficiency analysis. We study the empirical efficiency of WrapNet when vector operations are available. We extended the Gemmlowp library in [1] to implement matrix multiplications

Table 7: Time cost (ms) for typical 3×3 convolution layer in ResNet using different accumulator bitwidths.

Input size	Output	8-bit	32-bit
64x56x56	64	3.467	8.339
128x28x28	128	2.956	6.785
256x14x14	256	2.499	5.498
512x7x7	512	2.710	5.520

Table 8: Time cost (ms) for 3×3 convolution layer in ResNet with no vector instructions using bit packing.

Input size	Output	bit packing	naïve
64x56x56	64	29.80	83.705
128x28x28	128	23.86	80.557
256x14x14	256	21.71	86.753
512x7x7	512	20.41	87.671

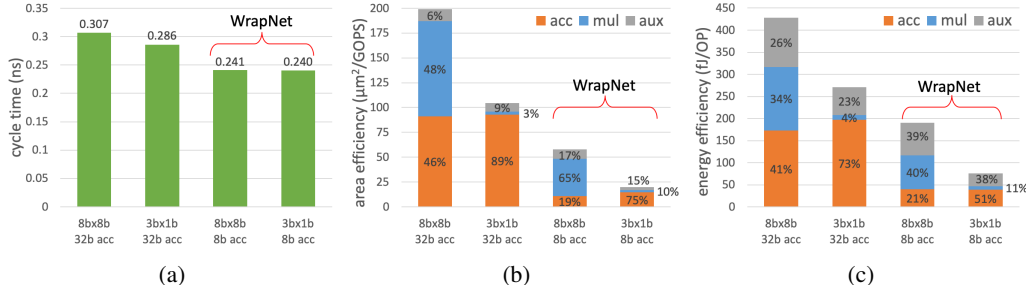


Figure 2: (a) Cycle time, (b) area and (c) energy efficiency for different MAC units implemented in 28nm CMOS. We consider 8-bit \times 8-bit or 3-bit \times 1-bit multipliers with 32-bit or 8-bit accumulators.

using 8-bit accumulators with AVX2 instructions. To demonstrate the efficiency of low-resolution accumulators, we compare our implementation to the AVX2 version of Gemmlowp, which uses 32-bit accumulators. We report the execution speed of both on various convolution layers of ResNet-18 in Table 7. From Table 7 we observe significant speed-ups ranging from $2\times$ for the $512 \times 7 \times 7$ block to $2.4\times$ for the $64 \times 56 \times 56$ block. The result provides solid evidence for the efficiency advantage of using low-resolution accumulators. We also remark that AVX2 lacks a single instruction that performs both multiplication and accumulation for 8-bit data, but it does have such instruction for 32-bit data. Thus, further acceleration can be achieved on systems like ARM where such combined instructions for 8-bit data are available.

Bit-packing results without vector operations. We study the efficiency of WrapNet when vector operations are unavailable. We implement a naïve for-loop based matrix multiplication, which uses buffer bit and logical operations introduced in Section 3.3 to form the baseline. We then pack four 8-bit integers into 32 bits, and report the execution speed of both implementations on various convolution layers of ResNet-18 in Table 8. The results in Table 8 show significant speed-ups ranging from $2.8\times$ to $4.3\times$. Such observations demonstrate our proposed approach to handle extra carry bits makes bit-packing viable and efficient, even when vector instructions are not available.

Hardware analysis. To illustrate the potential benefits of WrapNet for custom hardware accelerators, we have implemented a multiply-accumulate (MAC) unit in a commercial 28nm CMOS technology. The MAC unit consists of (i) a multiplier with an output register, (ii) an accumulator with its corresponding register, and (iii) auxiliary circuitry, namely input registers for the weights and activations, and global clock distribution circuitry. Please refer to Appendix C for the details. We have considered 8-bit \times 8-bit and 3-bit \times 1-bit hardware multipliers, as well as 32-bit and 8-bit accumulators, where the latter option is enabled by our WrapNet approach. Figure 2 shows post-layout results for the four combinations of the considered multipliers and accumulators.

Figure 2a shows that reducing the multiplier bitwidth decreases the cycle time by 7%; reducing the accumulator resolution from 32-bit to 8-bit further the cycle time by 16%. Our experiments show the accumulator is limiting the cycle time, as both 8-bit accumulator implementations achieve the same cycle time, regardless of the multiplier used. Figures 2b and 2c highlight the importance of reducing the accumulator’s resolution. When using an 8-bit \times 8-bit multiplier, the 32-bit accumulator already constitutes more than 40% of the area and energy of a MAC unit. Once the multiplier’s resolution reduces, the accumulator dominates area- and energy-efficiency. Thanks to WrapNet, we can reduce the accumulator resolution from 32-bit to 8-bit, thus reducing the accumulator’s area- and energy-efficiency by more than $8\times$ and $5\times$, respectively. Such gains in the accumulator correspond to reducing the total MAC unit’s area- and energy-efficiency by up to $5\times$ and $3\times$, respectively. We note that this analysis only considers the computation part of a hardware accelerator as this is where WrapNet has a significant impact—the memory sub-system will remain virtually the same, as existing methods already quantize the output activations to low-resolution before storing them in memory.

5 Conclusion

We have proposed WrapNet, a novel method to render neural networks resilient to integer overflow, which enables the use of low-resolution accumulators. We have demonstrated the effectiveness of

our adaptation on both CIFAR-10 and ImageNet. In addition, our custom GEMM kernel achieves $2.4\times$ acceleration over its standard library version, and our hardware exploration shows significant improvements in area- and energy-efficiency. Our hope is that hardware-aware architectures will enable deep learning applications on a wide range of platforms and mobile devices. Furthermore, with future innovations in GPU and data center technologies, we hope that WrapNet can provide further speed-ups by enabling inference using quarter-precision—a step forward in terms of performance from the currently available half-precision standard available on emerging GPUs.

Acknowledgement

The University of Maryland team was supported by the ONR MURI program, AFOSR MURI program, and the National Science Foundation DMS division. Addition support was provided by DARPA GARD, DARPA QED4RML, and DARPA YFA.

References

- [1] Google gemmlowp, 2016. <https://github.com/google/gemmlowp>.
- [2] Adrian Bulat and Georgios Tzimiropoulos. Xnor-net++: Improved binary neural networks. *arXiv preprint arXiv:1909.13863*, 2019.
- [3] Jungwook Choi, Pierce I-Jen Chuang, Zhuo Wang, Swagath Venkataramani, Vijayalakshmi Srinivasan, and Kailash Gopalakrishnan. Bridging the accuracy gap for 2-bit quantized neural networks (qnn). *arXiv preprint arXiv:1807.06964*, 2018.
- [4] Jungwook Choi, Zhuo Wang, Swagath Venkataramani, Pierce I-Jen Chuang, Vijayalakshmi Srinivasan, and Kailash Gopalakrishnan. Pact: Parameterized clipping activation for quantized neural networks. *arXiv preprint arXiv:1805.06085*, 2018.
- [5] Matthieu Courbariaux, Yoshua Bengio, and Jean-Pierre David. Binaryconnect: Training deep neural networks with binary weights during propagations. In *Advances in neural information processing systems*, pages 3123–3131, 2015.
- [6] Matthieu Courbariaux, Itay Hubara, Daniel Soudry, Ran El-Yaniv, and Yoshua Bengio. Binarized neural networks: Training deep neural networks with weights and activations constrained to+ 1 or-1. *arXiv preprint arXiv:1602.02830*, 2016.
- [7] Barry de Bruin, Zoran Zivkovic, and Henk Corporaal. Quantization of deep neural networks for accumulator-constrained processors. *Microprocessors and Microsystems*, 72:102872, 2020.
- [8] Yinpeng Dong, Renkun Ni, Jianguo Li, Yurong Chen, Jun Zhu, and Hang Su. Learning accurate low-bit deep neural networks with stochastic quantization. *arXiv preprint arXiv:1708.01001*, 2017.
- [9] Jongsoo Park et al. Fbgemm, 2018. <https://github.com/pytorch/FBGEMM>.
- [10] Ruihao Gong, Xianglong Liu, Shenghu Jiang, Tianxiang Li, Peng Hu, Jiazhen Lin, Fengwei Yu, and Junjie Yan. Differentiable soft quantization: Bridging full-precision and low-bit neural networks. In *Proceedings of the IEEE International Conference on Computer Vision*, pages 4852–4861, 2019.
- [11] Kaiming He, Xiangyu Zhang, Shaoqing Ren, and Jian Sun. Deep residual learning for image recognition. In *Proceedings of the IEEE conference on computer vision and pattern recognition*, pages 770–778, 2016.
- [12] Itay Hubara, Matthieu Courbariaux, Daniel Soudry, Ran El-Yaniv, and Yoshua Bengio. Binarized neural networks. In *Advances in neural information processing systems*, pages 4107–4115, 2016.
- [13] Benoit Jacob, Skirmantas Kligys, Bo Chen, Menglong Zhu, Matthew Tang, Andrew Howard, Hartwig Adam, and Dmitry Kalenichenko. Quantization and training of neural networks for efficient integer-arithmetic-only inference. In *Proceedings of the IEEE Conference on Computer Vision and Pattern Recognition*, pages 2704–2713, 2018.
- [14] Sangil Jung, Changyong Son, Seohyung Lee, Jinwoo Son, Jae-Joon Han, Youngjun Kwak, Sung Ju Hwang, and Changkyu Choi. Learning to quantize deep networks by optimizing

- quantization intervals with task loss. In *Proceedings of the IEEE Conference on Computer Vision and Pattern Recognition*, pages 4350–4359, 2019.
- [15] Alex Krizhevsky, Ilya Sutskever, and Geoffrey E Hinton. Imagenet classification with deep convolutional neural networks. In *Advances in neural information processing systems*, pages 1097–1105, 2012.
- [16] Fengfu Li, Bo Zhang, and Bin Liu. Ternary weight networks. *arXiv preprint arXiv:1605.04711*, 2016.
- [17] Hao Li, Soham De, Zheng Xu, Christoph Studer, Hanan Samet, and Tom Goldstein. Training quantized nets: A deeper understanding. In *Advances in Neural Information Processing Systems*, pages 5811–5821, 2017.
- [18] Xiaofan Lin, Cong Zhao, and Wei Pan. Towards accurate binary convolutional neural network. In *Advances in Neural Information Processing Systems*, pages 345–353, 2017.
- [19] Paulius Micikevicius, Sharan Narang, Jonah Alben, Gregory Diamos, Erich Elsen, David Garcia, Boris Ginsburg, Michael Houston, Oleksii Kuchaiev, Ganesh Venkatesh, et al. Mixed precision training. *arXiv preprint arXiv:1710.03740*, 2017.
- [20] Asit Mishra and Debbie Marr. Apprentice: Using knowledge distillation techniques to improve low-precision network accuracy. *arXiv preprint arXiv:1711.05852*, 2017.
- [21] Asit Mishra, Eriko Nurvitadhi, Jeffrey J Cook, and Debbie Marr. Wrpn: wide reduced-precision networks. *arXiv preprint arXiv:1709.01134*, 2017.
- [22] Fabrizio Pedersoli, George Tzanetakis, and Andrea Tagliasacchi. Espresso: Efficient forward propagation for binary deep neural networks. 2018.
- [23] Mohammad Rastegari, Vicente Ordonez, Joseph Redmon, and Ali Farhadi. Xnor-net: Imagenet classification using binary convolutional neural networks. In *European conference on computer vision*, pages 525–542. Springer, 2016.
- [24] Charbel Sakr, Naigang Wang, Chia-Yu Chen, Jungwook Choi, Ankur Agrawal, Naresh Shanbhag, and Kailash Gopalakrishnan. Accumulation bit-width scaling for ultra-low precision training of deep networks. *arXiv preprint arXiv:1901.06588*, 2019.
- [25] Marcel Simon, Erik Rodner, and Joachim Denzler. Imagenet pre-trained models with batch normalization. *arXiv preprint arXiv:1612.01452*, 2016.
- [26] Kuan Wang, Zhijian Liu, Yujun Lin, Ji Lin, and Song Han. Haq: Hardware-aware automated quantization with mixed precision. In *Proceedings of the IEEE conference on computer vision and pattern recognition*, pages 8612–8620, 2019.
- [27] Naigang Wang, Jungwook Choi, Daniel Brand, Chia-Yu Chen, and Kailash Gopalakrishnan. Training deep neural networks with 8-bit floating point numbers. In *Advances in neural information processing systems*, pages 7675–7684, 2018.
- [28] Shuchang Zhou, Yuxin Wu, Zekun Ni, Xinyu Zhou, He Wen, and Yuheng Zou. Dorefa-net: Training low bitwidth convolutional neural networks with low bitwidth gradients. *arXiv preprint arXiv:1606.06160*, 2016.
- [29] Chenzhuo Zhu, Song Han, Huizi Mao, and William J Dally. Trained ternary quantization. *arXiv preprint arXiv:1612.01064*, 2016.
- [30] Xiaotian Zhu, Wengang Zhou, and Houqiang Li. Adaptive layerwise quantization for deep neural network compression. In *2018 IEEE International Conference on Multimedia and Expo (ICME)*, pages 1–6. IEEE, 2018.

A Details of Carry Variance Reduction Regularizer

A.1 Carry Variance Calculation

With two’s complement representations for signed integers, a carry bit is generated in the following three cases: (i) addition of two negative numbers, (ii) addition of two positive numbers whose result exceeds the representation range, thus provoking integer overflow, and (iii) addition of a positive and a negative number whose result is a positive number. Dealing with these cases individually is complicated, but the calculation can be simplified by first reinterpreting the two’s complement representation as an unsigned integer. Carry bits resulting from accumulation of unsigned integers is easier to calculate as they can only happen in case (ii) as described above.

Since we only consider binary/ternary weights for bit-packing, carry bits can only be generated during accumulation, and not by multiplication. To produce a single output from a convolution, we must perform the accumulation $\sum_{i=1}^L \mathbf{v}_i$ of all entries of the vector $\mathbf{v} \in \mathbb{R}^L$. This is done by batching computations inside a b -bit register as follows. First, we bit-pack groups of numbers \mathbf{v}_i into several high-resolution registers. For example, let us consider the use of 32-bit registers to pack four $b = 8$ -bit numbers; then, we need to use $\lceil L/4 \rceil$ 32-bit registers to represent all L entries of \mathbf{v} . In the absence of vector instructions, the addition of these high-resolution registers will generate carry bits that will contaminate the adjacent bit-packed numbers. After all $\lceil L/4 \rceil$ additions take place, we add the 4 bit-packed numbers together to get a final result.

When one output feature is calculated by bit-backing as described above, the effect of carry bits is easy to simulate; accumulations can be done without accounting for carry bits during convolution, and then the carry bits can be added into the the final result after convolution takes place. If the total number of carries is large, this final correction can in turn produce new carry bits. Hence, we use Algorithm 1 to compute the total number of carry bits that are generated in an accumulation. The first equation simply reinterprets the signed representation to its unsigned counterpart u . Then, we compute the amount of carry bits c_i , as well as the result r_i remaining within the b -bit accumulator. Due to carry contamination, the carry bits c_i will be added to the result r_i , which may generate new carry bits c_{i+1} . We keep on adding the new carry bits to the accumulator until no new carry bits are generated. Note that, in real hardware at inference time, the most significant carry bit produced inside a register will be thrown away. For simplicity, our simulations during training accumulate all carry bits, including the most significant. We find that dropping the most significant carry during inference does not significantly impact testing.

Algorithm 1: Carry Amount Calculation

```

initialization  $\mathbf{v}, b$ ;
 $u = \sum_i ((\text{sign}(\mathbf{v}_i) + 1)/2) \mathbf{v}_i + ((-\text{sign}(\mathbf{v}_i) + 1)/2) (\mathbf{v}_i + 2^b)$ ;
 $c_i = u, r_i = 0, c = 0$ ;
while  $c_i \neq 0$  do
     $c_{i+1} = \lfloor (c_i + r_i)/2^b \rfloor$ ;
     $r_{i+1} = (c_i + r_i) \bmod 2^b$ ;
     $c = c + c_{i+1}$ ;
     $c_i = c_{i+1}, r_i = r_{i+1}$ 
end
return  $c$ 

```

Given the number of carry bits calculated during the inner product, the variance of the carry among a batch (b_s) of images is calculated as follows:

$$m_{b_s}(n^{i,l}) = \frac{1}{b_s} \left(\sum_{k=1}^{b_s} n_k^{i,l} \right), \quad (3)$$

$$\text{var}_{b_s}(n^{i,l}) = \frac{1}{b_s} \left(\sum_{k=1}^{b_s} (n_k^{i,l} - m_{b_s}(n^{i,l}))^2 \right), \quad (4)$$

where $n^{i,l}$ is the carry bit for the i -th neuron in l -th layer (assuming all the feature maps are vectorized). The estimated mean among all the images are learned by a moving average based on the mean of

batches (3). However, the sign and rounding function may have zero gradient almost everywhere. To make all the operations differentiable, we replace the sign function with a tanh function and we use a straight through estimator for rounding during the backward pass (gradient is identity). Then finally, our regularizer R^c will be the mean variance among all the neurons.

A.2 Training with Carry Variance Reduction Regularizer

Due to the large amount and high variance of carry-bit occurrences, it is hard to fine-tune our WrapNet even when using the carry variance reduction regularizer. The generated carry bits will be accumulated, which increases the overflow rate dramatically. In addition, the accumulation error will contaminate downstream computations and destroy accuracy. As a result, we fine-tune WrapNet with simulated carry bits layer by layer, starting from the layer which has the least carry variance. For the hybrid approach, we stop simulating the carry bit when we notice a significant accuracy drop; the remaining layers are trained using a buffer bit instead.

B Experimental Details

B.1 More Cyclic Functions

We compare two more “smooth” cyclic functions with our proposed cyclic activation function in Section 3. Specifically, we consider a cyclic absolute value function, and a ReLU-like function with transition slope k as alternative cyclic activations. Figure 3 illustrates the compared functions. We compare the results with and without a ReLU activation after batch normalization as well. Table 9 shows that retaining the ReLU activation after the batch normalization layer always achieves a better result, and that our proposed cyclic activation outperforms the other two choices.

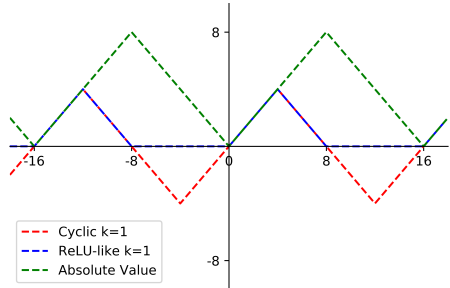


Figure 3: Example of the compared cyclic functions for a 4-bit accumulator.

Table 9: Results for different types of cyclic activation

Cyclic Function	ReLU	slope k	Accuracy(%)
Proposed	✓	2	90.52
Proposed		2	89.28
ReLU-like	✓	1	90.25
ReLU-like	✓	2	90.31
ReLU-like	✓	3	90.15
ReLU-like		1	88.62
ReLU-like		2	89.01
ReLU-like		3	88.53
Absolute	✓	–	90.17
Absolute		–	89.19

B.2 Full Overflow Penalty Results

Table 10 shows the results for fine-tuning our WrapNet with different coefficients for the overflow penalty. When applying the overflow penalty, the overflow rate decreases and we can achieve a higher

accuracy. In addition, when we apply the regularizer to a network with low-resolution accumulators that does not use our cyclic activation, the network still suffers from performance degradation unless a large coefficient is used. However, a strong penalty kills almost all of the overflow, which may limit the performance of a deep neural network.

Table 10: Comparison for fine-tuning network without cyclic activation and our WrapNet, with overflow penalty R^o .

Cyclic	R^o	Overflow rate (%)	Accuracy(%)
✓	0	6.29	90.52
✓	0.001	1.88	90.33
✓	0.01	1.24	90.81
✓	0.1	1.04	89.52
	0.01	5.91	64.69
	0.1	0.35	88.94
	1	0.06	90.26
	2	0.03	90.20

B.3 Training Details for Benchmark Results

For fair comparison, all our baselines (BWN/TWN, BWN-/TWN-QA) are fine-tuned from a pre-trained full-precision network. To obtain the benchmark results of our WrapNet, we follow a training pipeline, where we first warm-up our WrapNet with full-precision activations, and then we fine-tune the network for quantized activations. We set the transition slope $k = 2$, and the initial overflow rate $p = 5\%$. The overflow penalty coefficients for CIFAR-10 and ImageNet are 0.01 and 0.001, respectively.

For the CIFAR-10 results, we use ADAM as our optimizer with an initial learning rate of 0.001. For both warm-up and fine-tuning stages, we run 200 epochs, and the learning rate is divided by 10 every 60 epochs. For all the ImageNet results, we use SGD with momentum 0.9, weight decay 1×10^{-4} as our optimizer. We run 60 epochs for both warm-up and fine-tuning stages, where the initial learning rate is 0.01, which is divided by 10 at (20, 40, 50) epochs. We note that, due to depth of ResNet, we select a fixed quantization step-size for all the layers, where the average initial overflow rate is around 5%. As a result, the overflow penalty is also imposed during the warm-up stage for ResNet experiments.

C Hardware Analysis

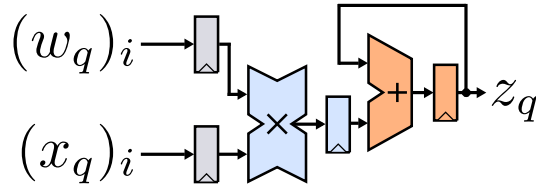


Figure 4: Multiply-accumulate (MAC) unit implemented for hardware analysis.

Figure 4 shows the multiply-accumulate (MAC) unit implemented in TSMC 28nm CMOS. The MAC unit multiplies two scalars and accumulates these products using an adder. To perform this functionality, the MAC unit is composed of multiplication, accumulation, and auxiliary circuitry, colored in Figure 4 with blue, orange, and gray, respectively. Clock distribution circuitry is not shown, but is included in our results as part of the auxiliary circuitry. To achieve lower cycle times (i.e., a faster operation frequencies), as well as to separate the multiplier’s and accumulator’s critical paths, we introduced a pipeline register between the multiplier and accumulator. For our implementation results, we consider this pipeline register as part of the multiplication circuitry.

We implemented the circuit in Figure 4 using different bitwidths for the multiplier (8-bit \times 8-bit or 3-bit \times 1-bit) and the accumulator (32-bit or 8-bit). When using the 8-bit \times 8-bit multiplier with the

32-bit accumulator, we use 16 bits for the multiplier’s output register to represent all possible products. When using the 8-bit \times 8-bit multiplier with the 8-bit accumulator, we use 8 bits for the multiplier’s output register, since the accumulator does not support larger bitwidths. When using the 3-bit \times 1-bit multiplier, we use 4 bits for the multiplier’s output register, regardless of the accumulator’s bitwidth.

The four different MAC units were synthesized using Synopsys Design Compiler (DC), and automatically placed-and-routed using Cadence Innovus. Power analysis was done using Cadence Innovus with stimuli-based post-layout simulations at 0.9V and 25°C in the typical-typical corner. For the stimuli, we used weights and activations extracted from a layer of the ResNet-18 network. Tables 11, 12, and 13 show the implementation results from Figure 2 in tabular form. Note that throughput is computed as 2/cycle time, as the MAC unit completes two operations (multiplication and accumulation) in a single clock cycle. However, in Figure 2, we decided to report cycle time so that, for all metrics presented (cycle time, area- and energy-efficiency), a lower value corresponds to a better performance. Note that circuits with a higher throughput (which corresponds, in this case, to a lower cycle time) often result in higher area and power consumption. As a matter of fact, dynamic power consumption is directly proportional to operation frequency (i.e., 1/cycle time). Thus, to perform a fair comparison, we have normalized the area and power reported in Table 11 by the throughput achieved, resulting in the area- and energy-efficiencies reported in Tables 12 and 13, respectively.

Table 11: Hardware implementation results for one multiply-accumulate (MAC) unit in 28nm CMOS

Bits			Cycle time (ns)	Throughput (Gops)	Cell area (μm^2)	Power (mW)
Activation	Weight	Accumulator				
8	8	32	0.307	6.51	1 298	2.78
3	1	32	0.286	6.99	732	1.90
8	8	8	0.241	8.30	479	1.58
3	1	8	0.240	8.33	164	0.63

Table 12: Area breakdown of one multiply-accumulate (MAC) unit in 28nm CMOS

Bits			Cell area efficiency ($\mu\text{m}^2/\text{Gops}$)			
Activation	Weight	Accumulator	Multiplier	Accumulator	Auxiliary	Total
8	8	32	96 (48%)	91 (46%)	12 (6%)	199 (100%)
3	1	32	3 (3%)	93 (89%)	9 (9%)	105 (100%)
8	8	8	37 (65%)	11 (19%)	10 (17%)	58 (100%)
3	1	8	2 (10%)	15 (75%)	3 (15%)	20 (100%)

Table 13: Energy breakdown of one multiply-accumulate (MAC) unit in 28nm CMOS

Bits			Energy efficiency (fJ/op)			
Activation	Weight	Accumulator	Multiplier	Accumulator	Auxiliary	Total
8	8	32	144 (34%)	173 (41%)	111 (26%)	428 (100%)
3	1	32	10 (4%)	197 (73%)	64 (23%)	271 (100%)
8	8	8	76 (40%)	40 (21%)	74 (39%)	190 (100%)
3	1	8	8 (11%)	39 (51%)	29 (38%)	76 (100%)

D Using more weight bits

Since ARM provides arithmetic operations that handle multiplication between various 8-bit numbers in parallel, we further conduct experiments in which more bits are used for weight quantization. Table 14 displays the classification accuracy, as well as the overflow rate of the final models. Surprisingly, in some cases, we may have a lower overflow rate even when using more bits for the weight quantization. We also collect the accuracy degradation from the full precision network. Our

results show that the best performance is achieved when we use 4-bit weights, which is close to the full-precision result (around 0.7% degradation).

Table 14: Results for WrapNet with more bits for weight quantization, where we use ternary weights for 2-bit.

Bits	Overflow Rate	Accuracy	Degradation
1	1.24%	90.81%	1.64%
2	0.12%	91.14%	1.31%
3	0.02%	91.55%	0.90%
4	0.04%	91.73%	0.72%
5	0.4%	91.20%	1.25%